Ledoux-convection in protoneutron stars – a clue to supernova nucleosynthesis ?

W. Keil, H.-Th. Janka, and E. Müller

Max-Planck-Institut für Astrophysik, Karl-Schwarzschild-Str. 1, Postfach 1523, 85740 Garching, Germany

July 5, 1996

Abstract. Two-dimensional (2D) hydrodynamical simulations of the deleptonization of a newly formed neutron star (NS) were performed. Driven by negative lepton fraction and entropy gradients, convection starts near the neutrinosphere about 20–30 ms after core bounce, but moves deeper into the protoneutron star (PNS), and after about one second the whole PNS is convective. The deleptonization of the star proceeds much faster than in the corresponding spherically symmetrical model because the lepton flux and the neutrino (ν) luminosities increase by up to a factor of two. The convection below the neutrinosphere raises the neutrinospheric temperatures and mean energies of the emitted ν's by 10–20%. This can have important implications for the supernova (SN) explosion mechanism and changes the detectable ν signal from the Kelvin-Helmholtz cooling of the PNS. In particular, the enhanced ν_e flux relative to the $\bar{\nu}_e$ flux during the early post-bounce evolution might solve the overproduction problem of certain elements in the neutrino-heated ejecta in models of type-II SN explosions.

Key words: supernovae: general – stars: neutron – elementary particles: neutrinos – turbulence – convection – hydrodynamics

1. Introduction

Convection in the newly formed NS might play an important role to explain the explosion of a massive star in a type-II SN. Epstein (1979) pointed out that not only entropy, S, inversions but also zones in the post-collapse core where the lepton fraction, Y_l, decreases with increasing radius tend to be unstable against Ledoux convection. Negative S and/or Y_l gradients in the neutrinospheric region and in the layers between the nascent NS and the weakening prompt shock front were realized in a variety of post-bounce SN models by Burrows & Lattimer (1988), and after shock stagnation in computations by Hillebrandt (1987) and more recently by Bruenn (1993), Bruenn & Mezzacappa (1994), and Bruenn et al. (1995). Despite of different equations of states (EOS), ν opacities, and ν transport methods, the development of negative Y_l and S gradients is common in these simulations and can also be found in PNS cooling models of Burrows & Lattimer (1987), Keil & Janka (1995), and Sumiyoshi et al. (1995).

Send offprint requests to: H.-Th. Janka

Convection above the neutrinosphere but below the neutrino-heated region can hardly be a direct help for the explosion (Bethe et al. 1987, Bruenn et al. 1995), whereas convectively enhanced lepton number and energy transport inside the neutrinosphere raise the ν luminosities and can definitely support neutrino-energized SN explosions (Bethe et al. 1987). In this context, Burrows (1987) and Burrows & Lattimer (1988) have discussed entropy-driven convection in the PNS on the basis of 1D, general relativistic (GR) simulations of the first second of the evolution of a hot, $1.4\,M_\odot$ PNS. Their calculations were done with a Henyey-like code using a mixing-length scheme for convective energy and lepton transport. Recent 2D models (Herant et al. 1994, Burrows et al. 1995, Janka & Müller 1996 and references therein) confirmed the possibility that convective processes can occur in the surface region of the PNS immediately after shock stagnation (“prompt convection”) for a period of at least several 10 ms. These models, however, have been evolved only over rather short times or with insufficient numerical resolution in the PNS or with a spherically symmetrical description of the core of the PNS that was in some cases even replaced by an inner boundary condition.

Mayle & Wilson (1988) and Wilson & Mayle (1988, 1993) demonstrated that convection in the nascent NS can be a crucial ingredient that leads to successful delayed explosions. With the high-density EOS and treatment of the ν transport used by the Livermore group, however, negative gradients of Y_l tend to be stabilized by positive S gradients (see, e.g., Wilson & Mayle 1989). Therefore they claim doubly diffusive neutron finger convection to be more important than Ledoux convection. Doubts about the presence of doubly diffusive instabilities, on the other hand, were recently raised by Bruenn & Dineva (1996). Bruenn & Mezzacappa (1994) and Bruenn et al. (1995) also come to a negative conclusion about the relevance of prompt convection in the neutrinospheric region. Although their post-bounce models show unstable S and Y_l stratifications, the mixing-length approach in their 1D simulations predicts convective activity inside and around the neutrinosphere to be present only for 10–30 ms after bounce and to have no significant impact on the ν fluxes and spectra when an elaborate multi-group flux-limited diffusion method is used for the ν transfer. Such conclusions seem to be supported by preliminary 2D simulations with the same input physics (Guidry 1996). These 2D models, however, still suffer from the use of an inner boundary condition at a fixed radius of 20–30 km.

From these differing and partly contradictory results it is evident that the question whether, where, when, and how long convection occurs below the neutrinosphere seems to be a matter of the EOS, of the core structure of the progenitor star, of the shock properties and propagation, and of the ν opacities and the ν transport description. In this Letter we compare 1D simulations with the first self-consistent 2D models that follow the evolution of the newly formed NS for more than a second, taking into account the GR gravitational potential and making use of a flux-limited equilibrium diffusion scheme that describes the transport of ν_e, $\bar{\nu}_e$, and ν_x (sum of ν_μ, $\bar{\nu}_\mu$, ν_τ, and $\bar{\nu}_\tau$) and is very good at high optical depths but only approximative near the PNS surface (Keil & Janka 1995). Our simulations demonstrate that Ledoux convection may continue in the PNS for a long time and can involve the whole star after about one second.

2. Numerical implementation

The simulations were performed with the explicit Eulerian hydrodynamics code *Prometheus* (Fryxell et al. 1989) that employs a Riemann-solver and is based on the Piecewise Parabolic Method (PPM) of Colella & Woodward (1984). A moving grid with 100 nonequidistant radial zones (initial outer radius $\sim 60\,\mathrm{km}$, final radius $\sim 20\,\mathrm{km}$) and with up to 60 angular zones was used, corresponding to a radial resolution of a few 100 m ($\lesssim 1\,\mathrm{km}$ near the center) and a maximum angular resolution of $1.5°$. In the angular direction periodic boundary conditions were imposed at $\pm 45°$ above and below the equatorial plane, and the stellar surface was treated as an open boundary where the velocity was calculated from the velocity in the outermost grid zone, the density profile was extrapolated according to a time-variable power law, and the corresponding pressure was determined from the condition of hydrostatic equilibrium. The *Prometheus* code was extended for the use of different time steps and angular resolutions in different regions of the star. Due to the extremely restrictive CFL condition for the hydrodynamics, the implicit ν transport was computed with typically 10 times larger time steps than the smallest hydrodynamics time step on the grid ($\sim 10^{-7}$ s) (Keil 1996).

Our simulations were started with the $\sim 1.1\,M_\odot$ (baryonic mass) central, dense part ($\rho \gtrsim 10^{11}\,\mathrm{g/cm^3}$) of the collapsed core of a $15\,M_\odot$ progenitor star (Woosley et al. 1988) that was computed to a time of about 25 ms after core bounce (i.e., a few ms after the stagnation of the prompt shock) by Bruenn (1993). Accretion was not considered but additional matter could be advected onto the grid through the open outer boundary. In the 2D run, Newtonian asphericity corrections were added to the spherically symmetrical GR gravitational potential: $\Phi_{\mathrm{2D}} \equiv \Phi_{\mathrm{1D}}^{\mathrm{GR}} + \left(\Phi_{\mathrm{2D}}^{\mathrm{N}} - \Phi_{\mathrm{1D}}^{\mathrm{N}}\right)$. This should be a sufficiently good approximation because convective motions produce only local and minor deviations of the mass distribution from spherical symmetry. Using the GR potential ensured that transients due to the mapping of Bruenn's (1993) relativistic 1D results to our code were very small. When starting our 2D simulation, the radial velocity (under conservation of the local specific total energy) was randomly perturbed in the whole PNS with an amplitude of 0.1%. The thermodynamics of the NS medium was described by the EOS of Lattimer & Swesty (1991) which yields a physically reasonable description of nuclear matter below about twice nuclear density and is thus suitable to describe the interior of the considered low-mass NS ($M_{\mathrm{ns}} \lesssim 1.2\,M_\odot$).

The ν transport was carried out in radial direction for every angular zone of the finest angular grid. Angular transport of neutrinos was neglected. This underestimates the ability of moving buoyant fluid elements to exchange lepton number and energy with their surroundings and is only correct if radial radiative and convective transport are faster. Moreover, ν shear viscosity was disregarded. For ν-n, p scattering and 3 flavors of nondegenerate ν and $\bar{\nu}$ in local thermal equilibrium with the matter one estimates at low densities ($\rho \lesssim 10^{14}\,\mathrm{g/cm^3}$) a dynamic shear viscosity of $\eta_\nu^{\mathrm{nd}} \sim 1.2 \cdot 10^{22} T_{10}^2/\rho_{14}\,\mathrm{g\,cm^{-1}s^{-1}}$ (van den Horn & van Weert 1981), and in degenerate nuclear matter $\eta_\nu^{\mathrm{d}} \sim 6.7 \cdot 10^{22} f(Y_p) T_{10}/\rho_{14}^{1/3}\,\mathrm{g\,cm^{-1}s^{-1}}$ (Thompson & Duncan 1993) when $T_{10} \equiv T/(10\,\mathrm{MeV})$ and $\rho_{14} \equiv \rho/(10^{14}\,\mathrm{g/cm^3})$. $f(Y_p) \approx 0.63 ... 1$ is a function of the proton fraction Y_p. With convective velocities $v_{\mathrm{c}} \sim 10^8\,\mathrm{cm/s}$ and length scales of convective mixing $l_{\mathrm{c}} \sim 10^5\,\mathrm{cm}$, one obtains Reynolds numbers $\mathcal{R}_\nu = v_{\mathrm{c}} l_{\mathrm{c}} \rho/\eta_\nu \sim 10^4 ... 10^5$ for typical temperatures and densities in the PNS, and corresponding viscous damping timescales of convective motions of the order of $t_\nu \sim \frac{1}{2} l_{\mathrm{c}}^2 \rho/\eta_\nu \approx$ 5–50 s. Neutrino viscosity is not extremely important on timescales of ~ 1 s and should not be able to suppress turbulent convection (Thompson & Duncan 1993, Burrows & Lattimer 1988).

The effective numerical viscosity of the PPM scheme is estimated from Eq. (3.6) in Porter & Woodward (1994) to be $\eta_{\mathrm{n}}/\rho \sim v_{\mathrm{c}} l_{\mathrm{c}} 10^y/(2\pi)^2$, which depends on the grid resolution via the parameter y defined as the ordinate in Fig. 1 of Porter & Woodward (1994). For structures of size $l_{\mathrm{c}}/(10^5\,\mathrm{cm}) \equiv l_{\mathrm{c},5} \gtrsim 1$ that are typically resolved by about 10 zones, and for flows with advective Courant numbers $C_{\mathrm{a}} \gtrsim 0.08$, Fig. 1 of Porter & Woodward (1994) leads to a dynamic shear viscosity of $\eta_{\mathrm{n}} \lesssim 5 \cdot 10^{23} \rho_{14} l_{\mathrm{c},5} v_{\mathrm{c},8}\,\mathrm{g\,cm^{-1}s^{-1}}$ when $v_{\mathrm{c},8} \equiv v_{\mathrm{c}}/(10^8\,\mathrm{cm/s})$. The corresponding Reynolds numbers are $\mathcal{R}_{\mathrm{n}} \sim (2\pi)^2 10^{-y} \gtrsim 2000$, and Eq. (3.5) of Porter & Woodward (1994) yields for the viscous damping timescale $t_{\mathrm{n}} \sim \frac{1}{2} \cdot 10^{-y} l_{\mathrm{c}}/v_{\mathrm{c}} \gtrsim 25\, l_{\mathrm{c},5}/v_{\mathrm{c},8}\,\mathrm{ms}$. This means that small structures represented by only a few grid cells will be affected by the numerical viscosity, but damping timescales for fluid motions on scales $l_{\mathrm{c}} \gtrsim 10^5\,\mathrm{cm}$ are still a factor $\frac{1}{2} \cdot 10^{-y} \gtrsim 25$ longer than the overturn timescales $t_{\mathrm{o}} \sim l_{\mathrm{c}}/v_{\mathrm{c}} \sim$ few ms.

3. Results

Convection can be driven by a radial gradient of the entropy per nucleon S and/or by a gradient of the lepton number per baryon Y_l (Epstein 1979) where Y_l includes contributions from e^- and e^+ and from ν_e and $\bar{\nu}_e$ if the latter are in equilibrium with the matter. Convective instability in the Ledoux approximation sets in when

$$\mathcal{C}_{\mathrm{L}}(r) \equiv \left(\frac{\partial\rho}{\partial S}\right)_{P,Y_l} \frac{\mathrm{d}S}{\mathrm{d}r} + \left(\frac{\partial\rho}{\partial Y_l}\right)_{P,S} \frac{\mathrm{d}Y_l}{\mathrm{d}r} > 0\,. \tag{1}$$

Initially, this criterion is fulfilled between $\sim 0.7\,M_\odot$ and $\sim 1.1\,M_\odot$ (black area in Fig. 1; see also Bruenn et al. 1995) and convective activity develops within $\sim 10\,\mathrm{ms}$ after the start of the 2D simulation. About 30 ms later the outer layers become convectively stable which is in agreement with Bruenn & Mez-

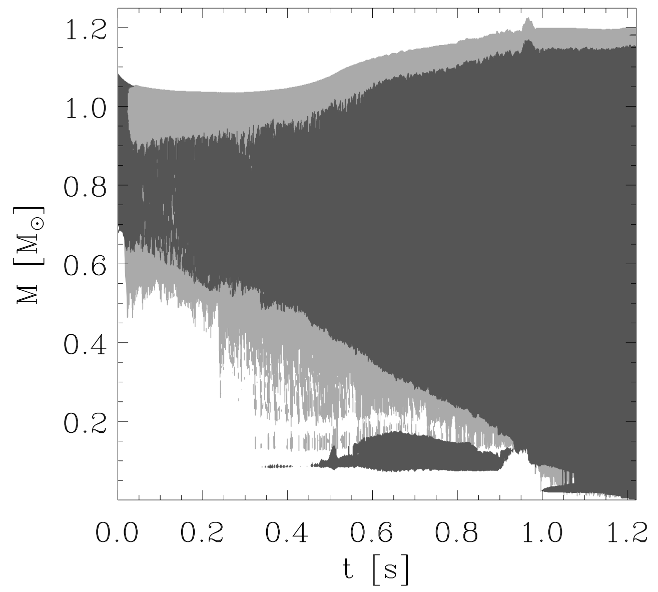

Fig. 1. Convective (baryon) mass region inside the PNS vs. time for the 2D simulation. Black indicates regions which are Ledoux unstable or only marginally stable, grey denotes over- and undershooting regions where $|v_\theta| > 10^7\,\mathrm{cm/s}$

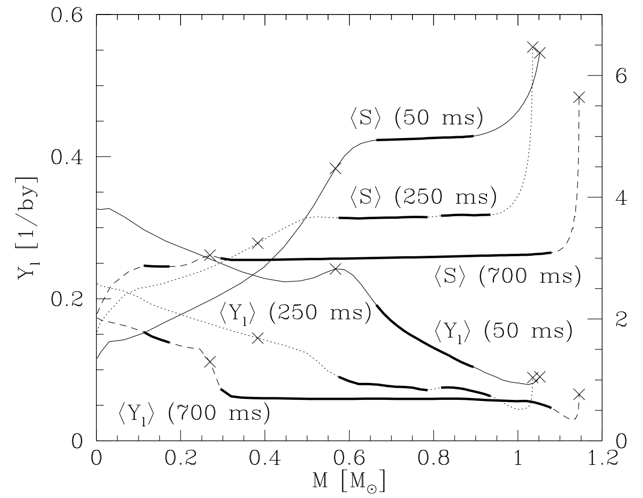

Fig. 2. Angle-averaged S and Y_l profiles in the PNS. Thick solid lines indicate regions that are unstable or only marginally stable against Ledoux convection, crosses mark boundaries of over- and undershooting regions where $|v_\theta| > 10^7\,\mathrm{cm/s}$

zacappa (1994). In our 2D simulation, however, the convectively unstable region retreats to mass shells $\lesssim\ 0.9\,M_\odot$ and its inner edge moves deeper into the neutrino-opaque interior of the star, following a steeply negative lepton gradient that is advanced towards the stellar center by the convectively enhanced deleptonization of the outer layers (Figs. 1 and 2). Note that the black area in Fig. 1 and the thick solid lines in Fig. 2 mark not only those regions in the star which are convectively unstable but also those *which are only marginally stable* according to the Ledoux criterion of Eq. (1) for angle-averaged S and Y_l, i.e., regions where $\mathcal{C}_\mathrm{L}(r) \geq a \cdot \max_r(|\mathcal{C}_\mathrm{L}(r)|)$ with $a = 0.05$ holds. For $a \lesssim 0.1$ the accepted region varies only little with a and is always embedded by the grey-shaded area where $|v_\theta| > 10^7\,\mathrm{cm/s}$. Yet, only sporadically and randomly appearing patches in the convective layer fulfill Eq. (1) rigorously. Figure 2 shows that the black region in Fig. 1 coincides with the layers where convective mixing flattens the S and Y_l gradients.

The convective pattern is extremely non-stationary and has most activity on large scales with radial coherence lengths of several km up to $\sim\ 10\,\mathrm{km}$ and convective "cells" of 20°–30° angular diameter, at some times even 45° (Fig. 3). Significant over- and undershooting takes place (grey regions in Fig. 1) and the convective mass motions create pressure waves and perturbations in the convectively stable NS interior and in the surface layers. The maximum convective velocities are $\sim 4 \cdot 10^8\,\mathrm{cm/s}$, but peak values of $\sim 10^9\,\mathrm{cm/s}$ can be reached. These velocities are typically 5–10% of the average sound speed in the star. The kinetic energy of the convection is several 10^{49} erg at $t \lesssim 1\,\mathrm{s}$ and climbs to $\sim 2 \cdot 10^{50}$ erg when the PNS is fully convective. Relative deviations of Y_l from the angular mean can be several 10% (even 100%) in rising or sinking buoyant elements, and for S can reach 5% or more. Rising flows always have larger Y_l *and* S than their surroundings. Corresponding temperature and density fluctuations are only $\sim$ 1–3%. Due to these properties and the problems to apply the Ledoux criterion with angle-averaged S and Y_l straightforwardly, we suspect that it is hardly possible to describe the convective activity with a mixing-length treatment in a 1D simulation.

Our 2D simulation shows that convection in the PNS can encompass the whole star within $\sim\ 1\,\mathrm{s}$ and can continue for at least as long as the deleptonization takes place, possibly even longer. A deleptonization "wave" associated with the convectively enhanced transport moves towards the center of the PNS. This reduces the timescale for the electron fraction Y_e to approach its minimum central value of about 0.1 from $\sim\ 10\,\mathrm{s}$ in the 1D case, where the lepton loss proceeds much more gradually and coherently, to only $\sim\ 1.2\,\mathrm{s}$ in 2D. With convection the entropy and temperature near the center rise correspondingly faster despite of a similar contraction of the star in 1D and 2D (Fig. 4). Convection increases the total lepton number flux and the ν luminosities by up to a factor of 2 (Fig. 5) and therefore the emitted lepton number N_l and energy E_ν rise much more rapidly (Fig. 4). The convective energy (enthalpy plus kinetic energy) flux dominates the diffusive ν energy flux in the convective mantle after $t\ \gtrsim\ 250\,\mathrm{ms}$ and becomes more than twice as large later. Since convection takes place somewhat below the surface, ν's take over the energy transport exterior to $\sim\ 0.9\,M_\odot$. Thus the surface ν flux shows relative anisotropies of only 3–4%, in peaks up to $\sim\ 10\%$, on angular scales of 10°–40°. Averaged over all directions, the neutrinospheric temperatures and mean energies $\langle\epsilon_{\nu_i}\rangle$ of the emitted ν_e and $\bar\nu_e$ are higher by 10–20% (Fig. 5).

4. Consequences and conclusions

The increase of the ν_e-luminosity relative to the $\bar\nu_e$-luminosity during $t\ \lesssim\ 0.4\,\mathrm{s}$ (Fig. 5) will raise Y_e^ej in the neutrino-heated SN ejecta. If weak equilibrium is established, α particles are absent, and $e^\pm$ captures can be ignored, captures of ν_e on n and $\bar\nu_e$ on p determine $Y_e^\mathrm{ej}\ \approx\ 1/\left[1 + (L_{\bar\nu_e}\langle\epsilon_{\bar\nu_e}\rangle)/(L_{\nu_e}\langle\epsilon_{\nu_e}\rangle)\right]$ (Qian & Woosley 1996). The luminosity ratio enters crucially, since $\langle\epsilon_{\bar\nu_e}\rangle/\langle\epsilon_{\nu_e}\rangle\ \approx\ T_{\bar\nu_e}/T_{\nu_e}$ does not change much due to convection (compare Fig. 5). The latter fact can be understood

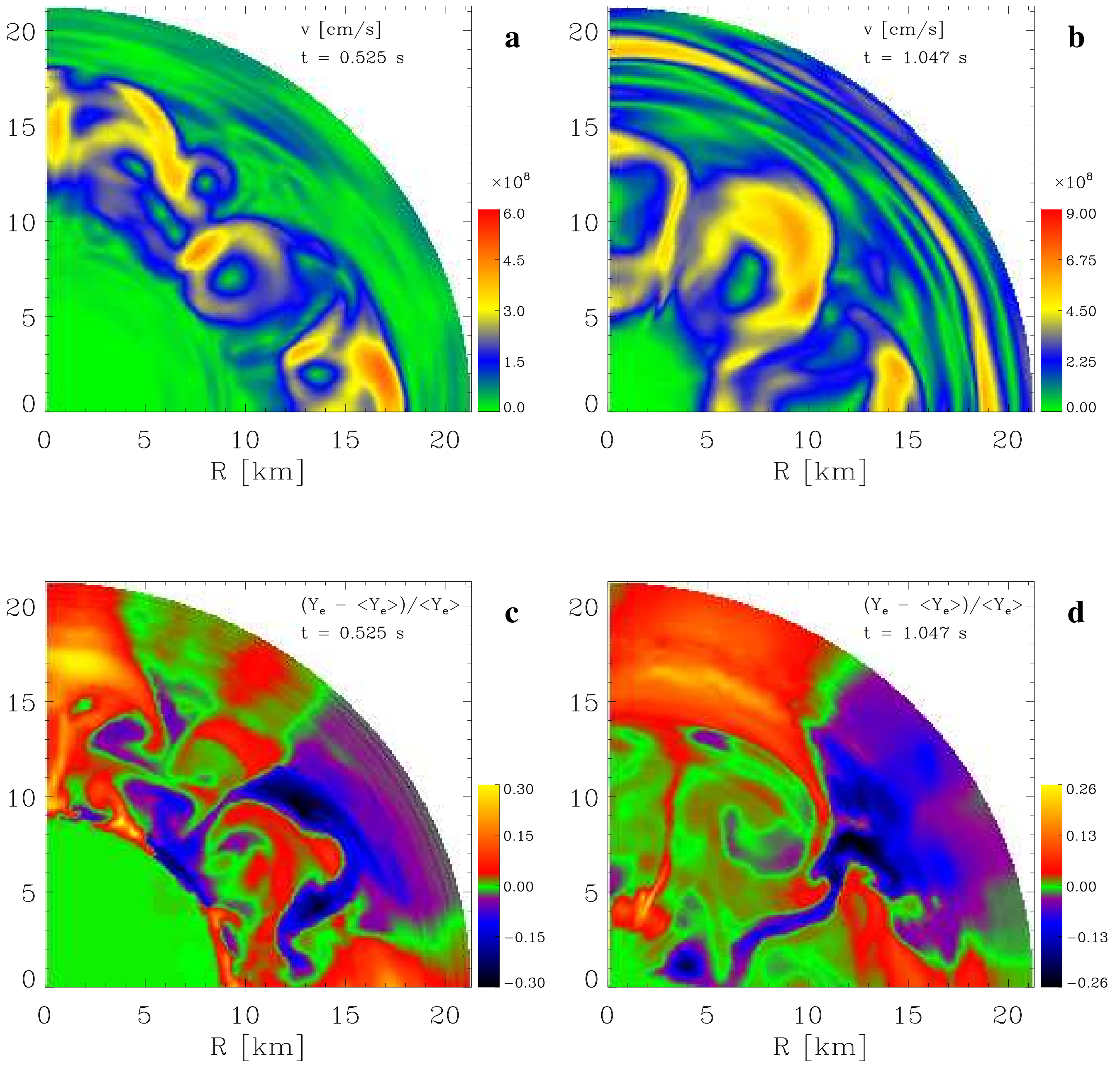

Fig. 3. Panels **a** and **b** show the absolute values of the velocity for the 2D simulation at times $t = 0.525$ s and $t = 1.047$ s, respectively, color-coded in units of 10^8 cm/s. The computation was performed in an angular wedge of $90°$ between $+45°$ and $-45°$ around the equatorial plane. The PNS has contracted to a radius of about 21 km at the given times. Panels **c** and **d** display the relative deviations of the electron fraction Y_e from the angular means $\langle Y_e \rangle$ at each radius for the same two instants. The maximum deviations are of the order of 30%. Lepton-rich matter rises while deleptonized material sinks in. Comparison of both times shows that the inner edge of the convective layer moves inward from about 8.5 km at $t = 0.525$ s to less than 2 km at $t = 1.047$ s

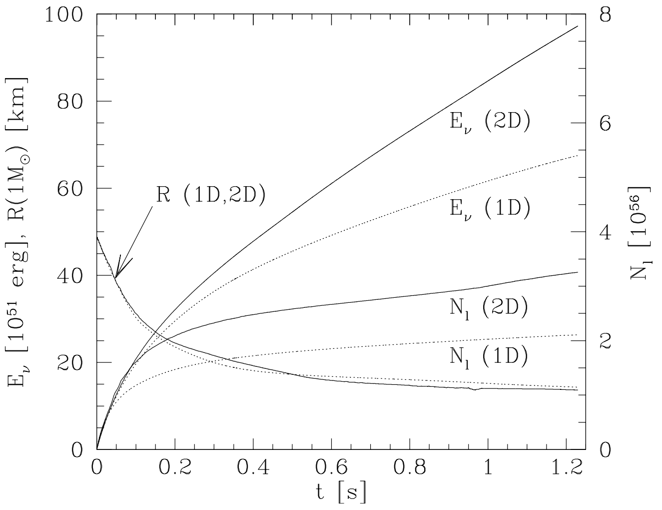

Fig. 4. Radius of the $M = 1\,M_{\odot}$ mass shell and total lepton number $N_{\rm l}$ and energy E_{ν} radiated away by ν's vs. time for the 2D (solid) and 1D (dotted) simulations

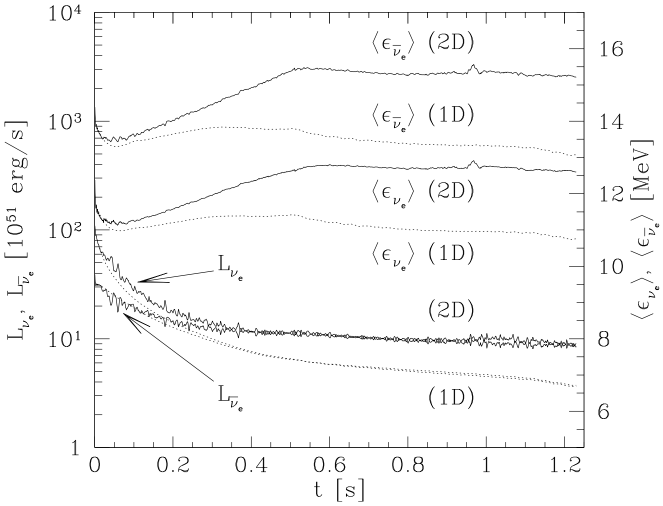

Fig. 5. ν_e and $\bar{\nu}_e$ luminosities and mean energies vs. time for the 2D simulation (solid) compared with the 1D run (dotted)

by an analytical neutrino Eddington atmosphere model (Schinder & Shapiro 1982) which yields for the temperatures T_{ν_i} of the ν_i energyspheres as functions of the effective temperature $T_{\rm eff}$: $T_{\nu_i} = \sqrt[4]{\xi_{\nu_i}/2}\,T_{\rm eff} \approx 4.6\,\sqrt[4]{\xi_{\nu_i}\mathcal{L}_{52}/r_6^2}$ MeV, where $\mathcal{L}_{52} \equiv (L_{\nu_e} + L_{\bar{\nu}_e})/(10^{52}\,{\rm erg/s})$, $r_6 \equiv r/(10^6\,{\rm cm})$. ξ_{ν_i} depends on the p and n abundance fractions, Y_p and $Y_n \approx 1 - Y_p$, in the NS atmosphere. For ν_e one gets $\xi_{\nu_e} \approx 1 + 1/(Y_n\sqrt{1 + 0.182Y_p/Y_n})$ and for $\bar{\nu}_e$ one finds $\xi_{\bar{\nu}_e} \approx 1 + 1/(Y_p\sqrt{1 + 0.210Y_n/Y_p})$. The ratio $T_{\bar{\nu}_e}/T_{\nu_e} = \sqrt[4]{\xi_{\bar{\nu}_e}/\xi_{\nu_e}}$ varies only weakly with the atmospheric composition. Moreover, one can derive that $Y_e^{\rm ej}$ increases if $f_{\rm n} > f_{\rm e}^{3/4}$ for $f_{\rm e} \equiv \mathcal{L}_{\rm 2D}/\mathcal{L}_{\rm 1D}$ and $f_{\rm n} \equiv \mathcal{N}_{\rm 2D}/\mathcal{N}_{\rm 1D}$ with $\mathcal{N} \equiv L_{\nu_e}/\langle\epsilon_{\nu_e}\rangle - L_{\bar{\nu}_e}/\langle\epsilon_{\bar{\nu}_e}\rangle$. This is fulfilled at times $t \lesssim 0.4\,{\rm s}$. The expected increase of $Y_e^{\rm ej}$ might help to avoid the overproduction of $N = 50$ nuclei in current SN models (see Hoffman et al. 1996, McLaughlin et al. 1996).

Future simulations of Ledoux convection in the PNS that include the progenitor star outside the nascent NS will have to reveal the effects on the SN explosion mechanism. PNS models with (baryonic) masses $M_{\rm ns} \approx 1.5\,...\,1.65\,M_{\odot}$ must be considered to investigate implications for the ν signal detected from SN 1987A. A more elaborate description of the ν transport and the use of different EOSs are also required. Convection in the PNS influences the structure of NS magnetic fields (Duncan & Thompson 1993), produces gravitational wave emission, and can cause NS recoils by anisotropic ν emission (Duncan & Thompson 1993). For non-stationary convection with typical coherence lengths $l_{\rm c} \sim 10^5\,{\rm cm}$ and overturn timescales $t_{\rm o} \lesssim R_{\rm ns}/v_{\rm c} \lesssim 10\,{\rm ms}$, one estimates a stochastic anisotropy of $\alpha \sim (l_{\rm c}/R_{\rm ns})\sqrt{t_{\rm o}/t_{\rm ns}} \lesssim 10^{-2}$ ($t_{\rm ns}$: NS cooling timescale) which leads to kick velocities $v_{\rm ns} \approx \alpha E_{\nu}/(M_{\rm ns}c)$ of a few $100\,{\rm km/s}$, dependent on the energy $E_{\nu} \lesssim \frac{3}{5}GM_{\rm ns}^2/R_{\rm ns}$ emitted anisotropically in neutrinos.

Acknowledgements. We would like to thank S.W. Bruenn for kindly providing us the post-collapse model to be used as initial model in our simulations. The computations were performed on the Cray-YMP 4/64 and the Cray-EL98 4/256 of the Rechenzentrum Garching.

References

Bethe H.A., Brown G.E., Cooperstein J., 1987, ApJ 332, 201

Bruenn S.W., 1993, in *Nuclear Physics in the Universe*, eds. M.W. Guidry and M.R. Strayer, IOP, Bristol, p. 31

Bruenn S.W., Mezzacappa A., 1994, ApJ 433, L45

Bruenn S.W., Mezzacappa A., Dineva T., 1995, Phys. Rep. 256, 69

Bruenn S.W., Dineva T., 1996, ApJ 458, L71

Burrows A., 1987, ApJ 318, L57

Burrows A., Hayes J., Fryxell B.A., 1995, ApJ 450, 830

Burrows A., Lattimer J.M., 1986, ApJ 307, 178

Burrows A., Lattimer J.M., 1988, Phys. Rep. 163, 51

Colella P., Woodward P.R., 1984, J. Comp. Phys. 54, 174

Epstein R.I., 1979, MNRAS 188, 305

Fryxell B.A., Müller E., Arnett W.D., 1989, MPA-Preprint 449, Garching

Guidry M.W., 1996, talk at the ECT workshop on *Physics of Supernovae and Neutron Stars*, Trento, Italy, June 3–14, 1996

Hillebrandt W., 1987, in *High Energy Phenomena around Collapsed Stars*, ed. F. Pacini, Reidel, Dordrecht, p. 73

Herant M., Benz W., Hix W.R., Fryer C.L., Colgate S.A., 1994, ApJ 435, 339

Hoffman R.D., Woosley S.E., Fuller G.M., Meyer B.S., 1996, ApJ 460, 478

van den Horn L.J., van Weert C.G., 1981, ApJ 251, L97

Janka H.-Th., Müller E., 1996, A&A 306, 167

Keil W., 1996, PhD Thesis, TU München (in preparation)

Keil W., Janka H.-Th., 1995, A&A 296, 145

Lattimer J.M., Swesty F.D., 1991, Nucl. Phys. A535, 331

Mayle R.W., Wilson J.R., 1988, ApJ 334, 909

McLaughlin G.C., Fuller G.M., Wilson J.R., 1996, ApJ, in press

Porter D.H., Woodward P.R., 1994, ApJS 93, 309

Qian Y.-Z., Woosley S.E., 1996, ApJ, in press

Schinder P.J., Shapiro S.L., 1982, ApJ 259, 311

Sumiyoshi K., Suzuki H., Toki H., 1995, A&A 303, 475

Thompson C., Duncan R.C., 1993, ApJ 408, 194

Wilson J.R., Mayle R.W., 1988, Phys. Rep. 163, 63

Wilson J.R., Mayle R.W., 1989, in *The Nuclear Equation of State, Part A*, eds. W. Greiner and H. Stöcker, Plenum Press, New York, p. 731

Wilson J.R., Mayle R.W., 1993, Phys. Rep. 227, 97

Woosley S.E., Pinto P.A., Ensman L., 1988, ApJ 324, 466

This article was processed by the author using Springer-Verlag LaTeX
A&A style file *L-AA* version 3.